OPEN

Machine Learning Quantitative Analysis of FDG PET Images of Medial Temporal Lobe Epilepsy Patients

Yen-Cheng Shih, MD,†‡ Tse-Hao Lee, MD,†§ Hsiang-Yu Yu, MD,*†‡ Chien-Chen Chou, MD,*†‡ Cheng-Chia Lee, MD, PhD,†‡|| Po-Tso Lin, MD,*†‡ and Syu-Jyun Peng, MD¶*

Purpose: ^{18}F-FDG PET is widely used in epilepsy surgery. We established a robust quantitative algorithm for the lateralization of epileptogenic foci and examined the value of machine learning of ^{18}F-FDG PET data in medial temporal lobe epilepsy (MTLE) patients.

Patients and Methods: We retrospectively reviewed patients who underwent surgery for MTLE. Three clinicians identified the side of MTLE epileptogenesis by visual inspection. The surgical side was set as the epileptogenic side. Two parcellation paradigms and corresponding atlases (Automated Anatomical Labeling and FreeSurfer aparc + aseg) were used to extract the normalized PET uptake of the regions of interest (ROIs). The lateralization index of the MTLE-associated regions in either hemisphere was calculated. The lateralization indices of each ROI were subjected for machine learning to establish the model for classifying the side of MTLE epileptogenesis.

Result: Ninety-three patients were enrolled for training and validation, and another 11 patients were used for testing. The hit rate of lateralization by visual analysis was 75.3%. Among the 23 patients whose MTLE side of epileptogenesis was incorrectly determined or for whom no conclusion was reached by visual analysis, the Automated Anatomical Labeling and aparc + aseg parcellated the associated ROIs on the correctly lateralized MTLE side in 100.0% and 82.6%. In the testing set, lateralization accuracy was 100% in the 2 paradigms.

Conclusions: Visual analysis of ^{18}F-FDG PET to lateralize MTLE epileptogenesis showed a lower hit rate compared with machine-assisted interpretation. While reviewing ^{18}F-FDG PET images of MTLE patients, considering the regions associated with MTLE resulted in better performance than limiting analysis to hippocampal regions.

Key Words: machine learning, ^{18}F-FDG PET, medial temporal lobe epilepsy, quantitative PET

(*Clin Nucl Med* 2022;47: 287–293)

Medial temporal lobe epilepsy (MTLE) is the most common drug-resistant epilepsy (DRE) in adults.[1] Compared with medical treatment alone, epilepsy surgery is considered an effective tool for seizure control for surgery-remediable patients with DRE.[2] ^{18}F-FDG PET has been used for epilepsy surgery assessments for a long time because the exhibition of regional cerebral hypometabolism in the ^{18}F-FDG PET process represents both the focus and projection areas of seizure activity.[3] FDG PET is helpful in lateralizing the side of epileptogenesis and predicting postoperative seizure outcomes.[4,5] Also, FDG PET data are valuable in the decision-making process regarding temporal lobe epilepsy (TLE) surgery, especially in patients with normal MRI findings or in conditions when ictal electroencephalogram (EEG) results are not consistent with MRI findings.[6] The concordance rate of ^{18}F-FDG PET in patients with TLE was 79% (95% confidence interval, 63%–92%) compared with the reference standard.[7] There are several reasons for the variable accuracy in determining the epileptogenic side in MTLE patients by FDG PET. For instance, PET scans are usually interpreted by visual inspection in clinical practice. There is interpersonal and intrapersonal variability in interpretation, especially in those who exhibited no significant differences in FDG uptake between bilateral temporal regions. Moreover, ipsilateral normal metabolism or hypermetabolism was noted in 7.8% of the patients with unilateral mesial temporal sclerosis (MTS).[8] Bilateral hypometabolism was reported in 10% to 30% of MTLE surgical cases of unilateral MTLE.[9,10] The inconsistent results with other presurgical examinations increase doubt about epileptogenic zone localization. This uncertainty usually leads to an intracranial study that increases invasiveness of the patients and the amount of medical resources required for the management of DRE. Glucose hypometabolism in TLE patients extends beyond the medial temporal structures.[11,12] We hypothesize that taking all related regions into account in an analysis increases the concordance rate of lateralization PET in MTLE patients. FDG PET also has the drawback of low spatial resolution for parcellation of the region of interest (ROI). Notably, quantitative measures have emerged in the interpretation of PET results in patients with epilepsy. There was a wide range of both sensitivity and specificity, ranging from 89% to 91%, among different methodologies.[13–16] Pertinently, artificial intelligence has increased its utility in epilepsy care. The number of analyses of quantitative functional neuroimaging by machine-assisted classifiers has greatly increased in clinical practice in recent years.[17] We conducted this study to establish a reliable and robust method to lateralize the side showing PET

Received for publication September 10, 2021; revision accepted November 20, 2021.

From the *Department of Neurology, Neurological Institute, Taipei Veterans General Hospital; †School of Medicine, National Yang Ming Chiao Tung University College of Medicine; ‡Brain Research Center, National Yang Ming Chiao Tung University; Departments of §Nuclear Medicine, and ||Neurosurgery, Neurological Institute, Taipei Veterans General Hospital; and ¶Professional Master Program in Artificial Intelligence in Medicine, College of Medicine, Taipei Medical University, Taipei, Taiwan.

Conflicts of interest and sources of funding: The authors have no conflicts of interest to declare. This work was supported by the Ministry of Science and Technology, Taiwan (MOST 110-2221-E-038-008, 110–2314-B-075–042, and 109–2314-B-075–053) and the National Health Research Institute (NHRI-EX109-10905N and NHRI-EX110-11006NC).

Correspondence to: Syu-Jyun Peng, PhD, Professional Master Program in Artificial Intelligence in Medicine, College of Medicine, Taipei Medical University, 19F, No. 172-1, Sec. 2, Keelung Rd, Da'an District, Taipei 10675, Taiwan. E-mail: sjpeng2019@tmu.edu.tw.

Supplemental digital content is available for this article. Direct URL citation appears in the printed text and is provided in the HTML and PDF versions of this article on the journal's Web site (www.nuclearmed.com).

ISSN: 0363-9762/22/4704–0287
DOI: 10.1097/RLU.0000000000004072

hypometabolism in patients with MTLE and examine the feasibility of this method in comparison with traditional visual inspection.

PATIENTS AND METHODS

Subjects

Subjects in the Model Training/Validation Set

We reviewed our database between July 2008 and June 2019 in Taipei Veterans General Hospital, Taiwan. The enrollment criteria were patients with drug-resistant MTLE who were to undergo epilepsy surgery with anterior temporal lobectomy or selective amygdalohippocampectomy. The presurgical workups included long-term video-EEG monitoring, high-resolution brain MRI, ^{18}F-FDG PET, and neuropsychological tests. The site of surgery was determined as the epileptogenic side. Only patients with a pathological diagnosis of MTS were enrolled. Patients with other pathological diagnoses, such as tumors, vascular lesions, and focal cortical dysplasia, were excluded. The seizure outcomes were obtained at 2 years after surgery.

Subjects in the Test Set

We established another group of 11 patients who would serve as the test set of the established model. These patients included those with MTLE who completed a stereotactic-EEG (sEEG) study and were waiting for subsequent resective surgery and those who underwent anterior temporal lobectomy or selective amygdalohippocampectomy beyond the period from July 2008 to June 2019. The epileptogenic side was determined according to the surgical side or the sEEG results.

^{18}F-FDG PET and MRI Acquisition Protocol

The patients fasted for at least 6 hours; fasting included avoidance of IV glucose-containing fluid. No clinical or EEG evidence of seizure onset was recorded for at least 2 hours before ^{18}F-FDG administration. If a patient's blood sugar was less than 150 mg/dL, the patient was intravenously administered ^{18}F-FDG at a dosage of 5 MBq/kg. Then, he or she would rest in a dim and quiet room and avoid reading with his or her eyes for approximately 30 minutes. No clinically overt seizure onset was noted during this 30-minute rest period. Afterward, each patient underwent brain PET in static acquisition mode for 15 minutes. If the brain PET study was performed before October 2019, PET images were acquired by the GE Healthcare Discovery STE PET/CT system. After October 2019, PET images were acquired by the GE Healthcare Discovery MI DR PET/CT or SIGNATM PET-MR system.

All MRI data (acquired by the Signa HDxt 3 T GE system, Signa HDxt 1.5 T GE system, or Siemens Magnetom 1.5 T system) were collected using an 8-channel phased-array neurovascular coil. Preoperative high-resolution 3-dimensional (3D) structural images were used for processing. The parameters used to acquire magnetization-prepared rapid acquisition with gradient echo (MPRAGE) images were as follows: repetition time, 6.228–8.988 milliseconds; echo time, 1.576–4.36 milliseconds; flip angle, 8–15 degrees; field of view, 256–256 mm; number of excitations, 1–2; and slice thickness, 1–1.5 mm.

^{18}F-FDG PET Lateralization by Visual Analysis

Two clinical neurologists and 1 nuclear medicine physician, all of whom were experienced in presurgical evaluation for DRE, reviewed the ^{18}F-FDG PET scan of the whole data set with visual inspection. The raters categorized the side of MTLE as either the left side, right side, or uncertain according to the significant hypometabolism of the medial temporal regions. If there were conflicting results among the raters, the outcome indicated by the majority of the raters was taken. Figure 1 shows an example of 2 patients with left MTLE whose results were both determined unanimously by the 3 physicians (Fig. 1A) and differed (Fig. 1B) among the 3 physicians.

Quantitative ^{18}F-FDG PET Machine Learning Model

The processing of the ^{18}F-FDG PET and MPRAGE images was implemented in MATLAB (MathWorks, Inc, Natick, MA) with applications of the Statistical Parametric Mapping program SPM12 (Functional Imaging Laboratory, Institute of Neurology, University College London, London, United Kingdom). We created 2 personalized atlases (the parcellated Automated Anatomical Labeling [AAL] atlas for Diffeomorphic Anatomical Registration through Exponential Lie Algebra [DARTEL] (Fig. 2) and the aparc + aseg atlas for FreeSurfer) that encompassed the anatomical labels to extract the normalized PET standardized uptake value of the ROI.

Step 1: Digital Imaging and Communications in Medicine to Neuroimaging Informatics Technology Initiative Conversion

The original DICOM (Digital Imaging and Communications in Medicine) file format of the ^{18}F-FDG PET and MPRAGE images was converted into the 3D NIfTI-1 (Neuroimaging Informatics Technology Initiative) file format. Because SPM12 uses NIFTI-1 as the file format of image data, this conversion facilitated the subsequent image preprocessing in SPM12.

Step 2: Resetting the MPRAGE and ^{18}F-FDG PET Image Orientation

The origin of the ^{18}F-FDG PET and MPRAGE images after the completion of step 1 was shifted to roughly align with the anterior commissure of the individual brain space. The purpose of this step was to improve the registering performance between the ^{18}F-FDG PET and MPRAGE images in SPM12, which occurred in the next step.

Step 3: Reregistering and Segmenting

The ^{18}F-FDG PET image was registered to the MPRAGE image by 3D voxel registration based on the normalized mutual information method. The MPRAGE image was a segmented brain tissue probability map including gray matter (GM, white matter [WM], and cerebrospinal fluid).

Step 4: ^{18}F-FDG PET Intensity Normalization and Smoothing

The current study proposes to use whole-brain GM as a reference region for intensity normalization of quantitative analysis of brain ^{18}F-FDG PET images. The whole-brain GM mask was defined as the 0.5 threshold and binarized probabilistic GM probability map. The intensity-normalized ^{18}F-FDG PET image was spatially smoothed with a Gaussian smoothing kernel of 8 mm full width at half maximum.

Step 5: Parcellating the Atlas

Paradigm I: Parcellating the AAL Atlas Using DARTEL

The new segment option in the SPM12 software package was applied to the MPRAGE image of the subject and the MPRAGE image of the AAL atlas to generate the imported tissue class image sets, that is, the imported GM image, the imported WM image, and the imported cerebrospinal fluid image. The imported tissue class image sets of the subject and AAL atlas were used to generate backward and forward flow fields as well as a series of template images through the DARTEL option embedded in SPM12. The AAL atlas was warped to match the shape of the subject based on the forward

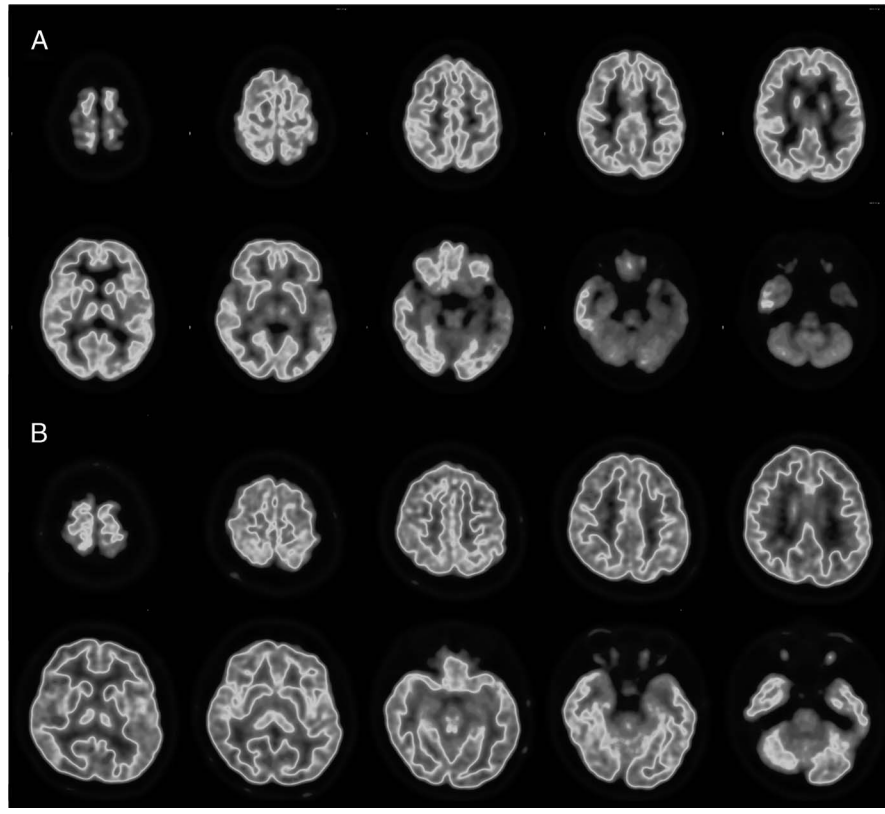

FIGURE 1. Analytic pipeline for the lateralization of epileptogenic foci interpretation: (1) resetting the MPRAGE and ^{18}F-FDG PET image orientation; (2) reregistering and segmenting; (3) normalizing and smoothing ^{18}F-FDG PET intensity; (4) generating imported tissue class images and flow fields to warp the AAL atlas into individual brain spaces; (5) selecting ROIs and calculating the mean uptake value; (6) acquiring machine learning interpretations of the lateralization of epileptogenic foci in MTLE patients (Frontal Sup Orb, superior orbital frontal gyrus; Frontal Mid Orb, middle orbital frontal gyrus; Frontal Inf Orb, inferior orbital frontal gyrus; Cingulum Post, posterior cingulate gyrus; Temporal Pole Sup, temporal pole of superior temporal gyrus; Temporal Pole Mid, temporal pole of middle temporal gyrus).

and backward flow fields to obtain a personalized anatomical atlas through the deformation option of SPM12. Then, 2 epileptologists (Y.C.S. and H.Y.Y.) and 1 nuclear medicine physician (T.H.L.) validated the anatomical parcellation accuracy of the deformed AAL atlases by comparing them to the individual ^{18}F-FDG PET images.

Paradigm II: Aparc + Aseg Atlas From FreeSurfer

In addition to paradigm I in which the parcellated AAL atlas was constructed, we created another personalized atlas (aparc + aseg atlas from FreeSurfer 7.1.1) that encompassed the anatomical labels to extract the normalized PET SUV of the ROIs. We ran recon-all

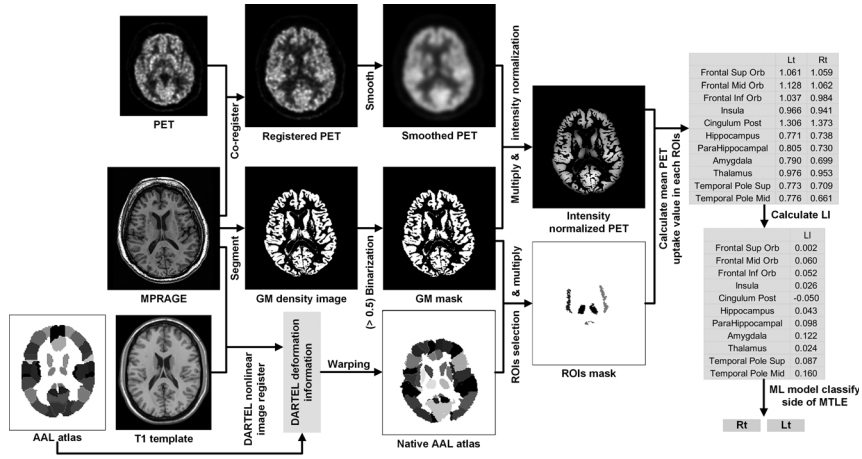

FIGURE 2. The comparison of patients with left MTLE presenting with concordant ^{18}F-FDG PET results (**A**) and nonconcordant FDG PET results (**B**) upon visual assessment.

commands from FreeSurfer using native-space MPRAGE and transformed segmentation into aparc + aseg atlas space to extract specific anatomical regions.

Step 6: Selecting ROIs and Calculating the Mean Uptake Value

We created 2 personalized atlases (the AAL atlas parcellated using DARTEL and the aparc + aseg atlas from FreeSurfer) that encompassed the anatomical labels that could be used to extract the normalized PET uptake of the ROIs. We were interested in the hippocampus and MTLE-associated regions. For the parcellated AAL atlas, the 11 MTLE-associated ROIs included the superior orbital frontal gyrus, middle orbital frontal gyrus, inferior orbital frontal gyrus, insula, posterior cingulate gyrus, hippocampus, parahippocampus, amygdala, thalamus, temporal pole of superior temporal gyrus, and temporal pole of middle temporal gyrus. For the aparc + aseg atlas, the 13 MTLE-associated ROIs were the thalamus, hippocampus, amygdala, entorhinal, lateral orbital gyrus, medial orbital gyrus, posterior cingulate gyrus, temporal pole, insular gyrus, parahippocampus, superior temporal gyrus, middle temporal gyrus, and inferior temporal gyrus. The mean SUV of each ROI was obtained by dividing the uptake count by the whole cerebral GM. For each subject, the corresponding mean uptake values of ^{18}F-FDG PET were calculated for bilateral ROIs. Also, the lateralization index was calculated for each ROI and was defined as $2 \times (L - R)/(L + R)$.

Step 7: Machine Learning Classification Modeling

Eleven lateralization indices for the parcellated AAL atlas and 13 lateralization indices for the aparc + aseg atlas were submitted to the training/validation set model to use in the classification of patients' MTLE sides. Seven machine learning models (including decision trees, discriminant analysis, logistic regression classifiers, naive Bayes classifiers, support vector machines, nearest neighbor classifiers, and ensemble classifiers) were used to train the model, and 10-fold cross-validation was used to establish the classification model by the classification learner app of MATLAB. After training each model in the classification learner app, we examined the overall accuracy, reported in percent, for each model. The validation accuracy score provides an estimate of a model's performance on new data compared with the training data. The model with the best validation accuracy score was selected for further clinical application.

Statistical Analysis

Descriptive statistics are presented as the count, percentage, and mean ± standard deviation. Mann-Whitney *U* tests and Fisher exact tests were used for the intergroup comparisons of continuous or categorical variables. The level of statistical significance was set at $P < 0.05$. The IBM Statistical Package for the Social Sciences (SPSS, version 26.0) was used for the data analysis.

Ethics

The study protocol was approved by the Institutional Review Board of Taipei Veterans General Hospital. All clinical investigations were conducted according to the principles expressed in the Declaration of Helsinki.

RESULTS

Patient Characteristics

Training/Validation Set

A total of 93 patients were enrolled in the training/validation set: 45 with left MTLE and 48 with right MTLE. There were 35 males and 58 females in the study cohort. The median seizure onset age was 13 years old (range, 0.5–48 years old), and the median age at surgery was 34 years old (range, 12–59 years old). After surgery, 2 patients were lost to follow-up within 2 years (one by 2 months and the other by 5 months). In the 91 patients who completed the postsurgical outcome evaluation, 77 patients achieved Engel classification I seizure outcomes (84.6%).

Test Set

There were 11 patients enrolled in the test set: 4 with left MTLE and 7 with right MTLE. There were 4 males and 7 females with a median seizure onset age of 18 years old (range, 0.5–40 years) in the study cohort. After the surgery, the surgical outcomes at 2 years were followed in 5 patients. There were no significant differences in sex, lesion side, onset age, age at operation or sEEG evaluation, seizure duration, or surgical outcome after surgery between the patients in the training/validation set and those in the test set. The detailed characteristics of the patients are shown in Table 1.

Lateralization of the MTLE Epileptogenic Side by Visual Analysis

Among the 93 cases in the training/validation set, the hit rate of lateralization by visual analysis was 75.3%. There were 23 patients for whom lateralization could not be performed by visual analysis of their ^{18}F-FDG PET images. There were 11 cases in the test set. The hit rate of lateralization by visual analysis was 72.7%. There were 3 patients for whom lateralization could not be performed by visual analysis of their ^{18}F-FDG PET images.

Performance of the Machine-Assisted Classifier Based on Associated ROIs

Machine-assisted MTLE epileptogenic side interpretation performance of different machine learning classifiers for the parcellated AAL atlas using DARTEL was evaluated. The nearest neighbor classifier model attained the best accuracy rate of 96.8% in these validation folds. In the aparc + aseg atlas of FreeSurfer, the support vector machine classifier model attained the best accuracy rate of 95.7% in these validation folds. There were no significant differences in performance between the 2 methods, as shown in Table 2.

Performance of the Machine-Assisted Classifier Based on Only the Hippocampus

The best accuracy rate of classifiers when the ROI was limited to the hippocampus was 94.6% and 95.7% in the parcellated AAL atlas and aparc + aseg, respectively, as shown in Table 3. The support vector machine classifier model attained the best accuracy rate of 94.6% in these validation folds. In the aparc + aseg atlas of FreeSurfer, the decision tree, support vector machine, and ensemble classifier models attained the best accuracy rate of 95.7% in these validation folds. Compared with a single ROI, there was slightly better performance on the lateralizing the MTLE epileptogenic side by using MTLE-associated ROIs in this cohort.

Model Evaluation in the Test Set

Model evaluation in the nearest neighbor classifier model for the parcellated AAL atlas using DARTEL attained an accuracy rate of 100.00% in the test set. In the aparc + aseg atlas of FreeSurfer, the support vector machine classifier model also attained an accuracy rate of 100.00% in the test set.

Clinical Implementation

For the 23 patients whose PET asymmetry could not be lateralized by visual analysis, the analysis of MTLE-associated ROIs provided a better lateralizing value compared with that obtained by analyzing the

TABLE 1. The Seizure-Related Characteristics of the Patients With Mesial Temporal Lobe Epilepsy

Demographics	Training/Validation Set (n = 93)	Test Set (n = 11)	Significance
Sex			1.0
Male	35 (37.6%)	4 (36.4%)	
Female	58 (62.4%)	7 (63.6%)	
Lesion side			0.53
Left	45 (48.4%)	4 (36.4%)	
Right	48 (51.6%)	7 (63.6%)	
Operation procedure		n = 7	0.028*
Anterior temporal lobectomy	26 (28.0%)	5 (71.4%)	
Selective amygdalohippocampectomy	67 (72.0%)	2 (28.6%)	
Outcome	n = 91	n = 5	0.963
Engel class I	77 (84.6%)	4 (80%)	
Engel class II	12 (13.2%)	1 (20%)	
Engel class III	1 (1.1%)	0 (0%)	
Engel class IV	1 (1.1%)	0 (0%)	
Demographics	Mean ± SD, y		
Age at seizure onset	15.69 ± 10.33	16.50 ± 12.97	0.95
Age at operation or sEEG	34.61 ± 11.17	32.09 ± 10.54	0.45
Seizure duration	18.92 ± 11.99	15.59 ± 9.19	0.44

*$P < 0.05$.

hippocampus alone. Among the 23 patients whose sides of MTLE epileptogenesis were incorrectly determined or for whom no conclusion was reached by visual analysis, the AAL and aparc + aseg parcellated hippocampus models correctly lateralized the side of MTLE epileptogenesis in the same 87.0%. When the MTLE-associated ROI model was used, the side of MTLE epileptogenesis was correctly lateralized in 100.0% and 82.6% of the patients, respectively.

DISCUSSION

This study aimed to establish a reliable automatic method to lateralize the lesion side of patients with MTLE using FDG PET. The machine-assisted quantitative method of FDG PET in MTLE patients showed a higher accuracy than the traditional method of visual analysis. We used 2 different parcellation methods, the DARTEL method and the aparc + aseg atlas of FreeSurfer, for machine-assisted MTLE epileptogenic side interpretation. These 2 methods had equally high accuracy (96.8% and 95.7%, respectively) in the validation set. We further used these 2 methods to analyze 23 patients whose lesion side could not be lateralized through visual analysis. The DARTEL method had an advantage over the FreeSurfer method among these patients.

FDG PET is a powerful tool for epileptogenic focus lateralization. Pustina et al[18] investigated the asymmetries shown on FDG PET images, cortical thickness demonstrated on MRI scans, and WM anisotropy indicated by diffusion tensor imaging in 58 patients with TLE and found that PET asymmetries alone formed the best predictive model. Both visual[19] and SPM[13] analysis studies have shown that patients with MTLE typically have glucose hypometabolism lesions on the ipsilateral side. Also, the traditional visual analysis method has higher variability.[20] Previous studies showed that radiology reports and the epilepsy surgery conference consensus differ 31% of the time in FDG PET studies.[21] In this study, the accuracy of visual analysis by 3 physicians was 75.3%. Moreover, previous studies showed that the accuracy of FDG PET by visual analysis in overall intractable epilepsy is 85% (86% in patients with good outcomes, 58% in patients who need invasive studies),[22] and the accuracy in MTLE patients is 64%.[14] The visual analysis was frequently disturbed, whereas the asymmetry of glucose metabolism was not obvious in these patients. Bilateral temporal hypometabolism in patients with MTLE might be associated with a shorter duration from the last seizure to the PET scan.[10] In unilateral MTS patients, the surgical outcomes of patients with bilateral temporal lobe hypometabolism were similar to those of patients with unilateral

TABLE 2. Performance of the Machine-Assisted Classifier Based on Associated ROIs

	Accuracy (%)	
Classifiers	Parcellated AAL	Aparc + Aseg
Decision tree	93.5	90.3
Discriminant analysis	95.7	93.5
Logistic regression	88.2	89.2
Naive Bayes classifier	94.6	93.5
Support vector machine	95.7	95.7
Nearest neighbor classifier	96.8	95.7
Ensemble classifier	95.7	93.5

TABLE 3. Performance of the Machine-Assisted Classifier Based on Only the Hippocampus

	Accuracy (%)	
Classifiers	Parcellated AAL	Aparc + Aseg
Decision tree	91.4	95.7
Discriminant analysis	92.5	92.5
Logistic regression	92.5	93.5
Naive Bayes classifier	92.5	92.5
Support vector machine	94.6	95.7
Nearest neighbor classifier	92.5	94.6
Ensemble classifier	93.5	95.7

temporal hypometabolism.[9,23] Furthermore, another scenario that might mislead the visual analysis is hypermetabolism in MTLE patients. False lateralization of TLE with FDG PET has been reported[24,25] when patients experienced frequent subclinical seizures on the side of MTLE epileptogenesis. To avoid false information prompted by the hypermetabolic hippocampus, we included MTLE-associated ROIs to improve lateralization accuracy. Pertinently, glucose hypometabolism has been demonstrated in regions of the ipsilateral temporal and extratemporal regions, including the amygdalohippocampal complex, parahippocampal gyrus, temporal pole, orbitofrontal cortex, insula, posterior and anterior cingulate gyrus, and thalamus.[21]

Quantification of ^{18}F-FDG brain PET might be helpful in defining the epileptogenic zone, especially when MRI findings are negative. This method also complements conventional visual analysis by improving the sensitivity for epileptogenic lesion detection.[7] Several published studies have attempted to increase the accuracy of lateralization using a quantitative method of FDG PET interpretation. Kim et al[13] used the SPM method to examine presurgical PET results in patients with TLE by using PET scan of normal subjects as reference. The accuracy of hypometabolism of the epileptogenic side in FDG PET scans was 76% (sensitivity of 89% and specificity of 91%).[13] However, quantitative FDG brain PET of normal subjects has the limitation of a lack of standardization of the brain state, age, and sex among the subjects, which may result in large physiological variability and less sensitivity in the detection of glucose metabolic abnormalities.[26] We compared the FDG PET of both sides of the medial temporal lobe in the same individual to reduce interindividual variability. In this study, we used high-resolution brain MRI for image segmentation. Because of the relatively low resolution of FDG PET images, direct segmentation of PET images would result in a severe partial volume effect. Also, brain MRI scans have higher resolution than brain PET images and could minimize the partial volume effect. Moreover, during parcellation of the high-resolution brain MRI scans, we created a personalized atlas, which could provide more accurate anatomical labels of individuals. The normalized PET SUV was then applied to the ROI, which could also increase the accuracy of PET quantitation.[27]

In the quantification of FDG PET, manual segmentation of brain MRI scans is still the criterion standard. However, this method requires repetitive tasks, is time-consuming, and is based on the experience of physicians.[28] Many methods of total automated segmentation have been developed to solve these problems and have achieved various levels of accuracy (Dice similarity coefficients, 0.68–0.94).[29] Grimm et al[30] compared automatic segmentation, including that achieved by VBM8 and FreeSurfer version 5.0, with manual segmentation in the volume of the amygdala and hippocampus in 92 patients enrolled in a posttraumatic stress disorder disease study. The authors concluded that the correlation between automatic and manual segmentation was high for the hippocampus and lower for the amygdala (Pearson correlation coefficients, 0.58–0.76 and 0.45–0.59, respectively). Compared with manual segmentation, VBM8 and FreeSurfer segmentation have comparable performance.

Hu et al[31] also used automated quantitative analyses of hippocampal volume and glucose uptake to lateralize the lesion side in patients with MTLE. The authors used the MPRAGE sequence in FreeSurfer software for automatic segmentation of brain images. The study showed higher sensitivity in quantitative methods than visual assessment methods (98.15% and 81.48%, respectively, $P = 0.008$). The quantitative measurement of FDG PET uptake in the hippocampus was more sensitive than hippocampal volumetry by T1 sequencing in MRI scans, although there was no statistical significance (98.15% and 92.59%, respectively, $P = 0.343$). However, this study only interpreted quantitative hippocampal images and did not consider the epileptogenic network. Furthermore, the study did not examine the performance of quantitative analysis on data that could not be well lateralized by visual analysis. In our study, we found that the quantification methods could detect 87%

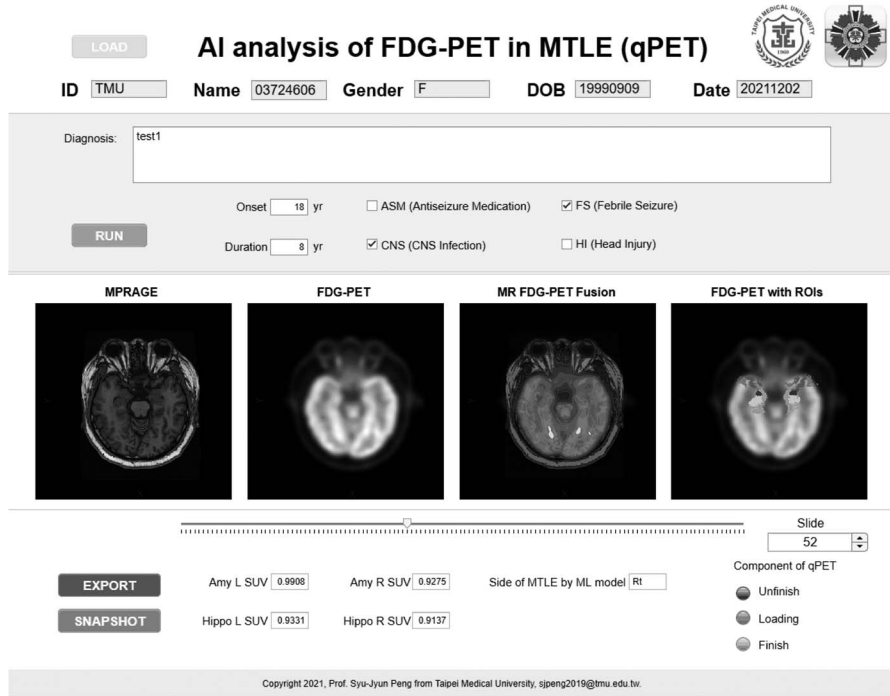

FIGURE 3. Overview of the qPET tool, including LOAD, RUN, EXPORT, and SNAPSHOT functions. LOAD initiates the input of MPRAGE and ^{18}F-FDG PET DICOM data. RUN initiates the machine-assisted quantitative procedure of FDG PET on the lateralizing side of MTLE patients. EXPORT outputs the analysis results, including the bilateral amygdala and hippocampus SUV and lateralization side of MTLE patients. SNAPSHOT captures an image of the processed ^{18}F-FDG PET and qPET GUI results page.

of the visual analysis failure cases. In addition to FreeSurfer segmentation, we also used the DARTEL method. The lateralization index obtained from these 2 methods could be well analyzed using the classifiers. The performance was similar in 2 methods. More specifically, for clinical practice, the DARTEL method has an advantage of a short computing time (25 minutes for DARTEL vs 6 hours for FreeSurfer) and could be performed on either Windows or MacOS systems. We also developed a graphical user interface (GUI), so that this method could be incorporated into clinical practice.

The study had some limitations. First, we used the surgical side as a standard of determination of the epileptogenic side. Disparate interpretations could arise in the evaluation of patients who were not seizure-free after surgery. We examined postoperative EEG data in 2 patients who did not achieve favorable surgical outcomes (1 Engle class III and 1 Engle class IV). Also, the postoperative epileptiform discharges were localized on the side of surgery, which suggested a more widely distributed epileptogenic network. There was no evidence that the recurring seizures were from the contralateral side. Second, this was a single-center study with a relatively small sample size. A multicenter study with larger sample sizes is needed to test the model we developed. We developed a GUI to facilitate the artificial intelligence (AI) analysis of FDG PET (qPET) (Fig. 3, Video 1, http://links.lww.com/CNM/A363), which could be conducted at different epilepsy centers. The performance of this algorithm could consequently be examined. Third, all the enrolled patients had drug-resistant MTLE. Moreover, the usage of the proposed model for patients with other epileptogenic foci might need further evaluation.

CONCLUSIONS

In this research, we developed a machine learning quantitative method of evaluating ^{18}F-FDG PET data to determine the lateralization of the side of MTLE epileptogenesis. The machine learning classifier was adopted to deliver an AI tool that is capable of extracting image features from the ^{18}F-FDG PET data and classifying normalized PET uptake of the ROI of ^{18}F-FDG PET images into lateralization epileptogenic foci. Image preprocessing on the patient data emphasized the critical information pertaining to successful lateralization epileptogenic foci interpretation from ^{18}F-FDG PET images. The validation folds achieved approximately 96.0% accuracy in lateralization of epileptogenic foci interpreted from the parcellated AAL atlas using DARTEL deformation or the aparc + aseg atlas from FreeSurfer. The proposed AI-based lateralization epileptogenic foci interpretation method could provide assistance in the preoperative diagnosis of epilepsy surgery with ^{18}F-FDG PET scans, which is highly accurate and readily available.

ACKNOWLEDGMENTS

The authors thank the National Core Facility for Biopharmaceuticals (MST 109-2740-B-492-001) for their support and the National Center for High-Performance Computing of National Applied Research Laboratories in Taiwan for providing computational and storage resources.

REFERENCES

1. Blumcke I. Neuropathology of focal epilepsies: a critical review. *Epilepsy Behav*. 2009;15:34–39.
2. Wiebe S, Blume WT, Girvin JP, et al. A randomized, controlled trial of surgery for temporal-lobe epilepsy. *N Engl J Med*. 2001;345:311–318.
3. Rathore C, Dickson JC, Teotonio R, et al. The utility of ^{18}F-fluorodeoxyglucose PET (FDG PET) in epilepsy surgery. *Epilepsy Res*. 2014;108:1306–1314.
4. Theodore WH, Sato S, Kufta C, et al. Temporal lobectomy for uncontrolled seizures: the role of positron emission tomography. *Ann Neurol*. 1992;32:789–794.
5. Willmann O, Wennberg R, May T, et al. The contribution of ^{18}F-FDG PET in preoperative epilepsy surgery evaluation for patients with temporal lobe epilepsy A meta-analysis. *Seizure*. 2007;16:509–520.
6. Uijl SG, Leijten FS, Arends JB, et al. The added value of [^{18}F]-fluoro-D-deoxyglucose positron emission tomography in screening for temporal lobe epilepsy surgery. *Epilepsia*. 2007;48:2121–2129.
7. Niu N, Xing H, Wu M, et al. Performance of PET imaging for the localization of epileptogenic zone in patients with epilepsy: a meta-analysis. *Eur Radiol*. 2021;31:6353–6366.
8. Talanow R, Ruggieri P, Alexopoulos A, et al. PET manifestation in different types of pathology in epilepsy. *Clin Nucl Med*. 2009;34:670–674.
9. Kim MA, Heo K, Choo MK, et al. Relationship between bilateral temporal hypometabolism and EEG findings for mesial temporal lobe epilepsy: analysis of ^{18}F-FDG PET using SPM. *Seizure*. 2006;15:56–63.
10. Tepmongkol S, Srikijvilaikul T, Vasavid P. Factors affecting bilateral temporal lobe hypometabolism on ^{18}F-FDG PET brain scan in unilateral medial temporal lobe epilepsy. *Epilepsy Behav*. 2013;29:386–389.
11. Chassoux F, Artiges E, Semah F, et al. ^{18}F-FDG-PET patterns of surgical success and failure in mesial temporal lobe epilepsy. *Neurology*. 2017;88:1045–1053.
12. Kumar A, Chugani HT. The role of radionuclide imaging in epilepsy, part 1: sporadic temporal and extratemporal lobe epilepsy. *J Nucl Med*. 2013;54:1775–1781.
13. Kim YK, Lee DS, Lee SK, et al. Differential features of metabolic abnormalities between medial and lateral temporal lobe epilepsy: quantitative analysis of (18)F-FDG PET using SPM. *J Nucl Med*. 2003;44:1006–1012.
14. Peter J, Houshmand S, Werner TJ, et al. Novel assessment of global metabolism by ^{18}F-FDG-PET for localizing affected lobe in temporal lobe epilepsy. *Nucl Med Commun*. 2016;37:882–887.
15. Van Bogaert P, Massager N, Tugendhaft P, et al. Statistical parametric mapping of regional glucose metabolism in mesial temporal lobe epilepsy. *Neuroimage*. 2000;12:129–138.
16. Mayoral M, Marti-Fuster B, Carreno M, et al. Seizure-onset zone localization by statistical parametric mapping in visually normal (18) F-FDG PET studies. *Epilepsia*. 2016;57:1236–1244.
17. Abbasi B, Goldenholz DM. Machine learning applications in epilepsy. *Epilepsia*. 2019;60:2037–2047.
18. Pustina D, Avants B, Sperling M, et al. Predicting the laterality of temporal lobe epilepsy from PET, MRI, and DTI: a multimodal study. *Neuroimage Clin*. 2015;9:20–31.
19. Henry TR, Mazziotta JC, Engel J Jr. Interictal metabolic anatomy of mesial temporal lobe epilepsy. *Arch Neurol*. 1993;50:582–589.
20. Kerr WT, Nguyen ST, Cho AY, et al. Computer-aided diagnosis and localization of lateralized temporal lobe epilepsy using Interictal FDG-PET. *Front Neurol*. 2013;4:31.
21. Kojan M, Dolezalova I, Koritakova E, et al. Predictive value of preoperative statistical parametric mapping of regional glucose metabolism in mesial temporal lobe epilepsy with hippocampal sclerosis. *Epilepsy Behav*. 2018;79:46–52.
22. Won HJ, Chang KH, Cheon JE, et al. Comparison of MR imaging with PET and ictal SPECT in 118 patients with intractable epilepsy. *AJNR Am J Neuroradiol*. 1999;20:593–599.
23. Joo EY, Lee EK, Tae WS, et al. Unitemporal vs bitemporal hypometabolism in mesial temporal lobe epilepsy. *Arch Neurol*. 2004;61:1074–1078.
24. Sperling MR, Alavi A, Reivich M, et al. False lateralization of temporal lobe epilepsy with FDG positron emission tomography. *Epilepsia*. 1995;36:722–727.
25. Tafti BA, Mandelkern M, Berenji GR. Subclinical seizures as a pitfall in ^{18}F-FDG PET imaging of temporal lobe epilepsy. *Clin Nucl Med*. 2014;39:819–821.
26. Traub-Weidinger T, Muzik O, Sundar LKS, et al. Utility of absolute quantification in non-lesional extratemporal lobe epilepsy using FDG PET/MR imaging. *Front Neurol*. 2020;11:54.
27. Ruan W, Sun X, Hu X, et al. Regional SUV quantification in hybrid PET/MR, a comparison of two atlas-based automatic brain segmentation methods. *EJNMMI Res*. 2020;10:60.
28. Carmichael OT, Aizenstein HA, Davis SW, et al. Atlas-based hippocampus segmentation in Alzheimer's disease and mild cognitive impairment. *Neuroimage*. 2005;27:979–990.
29. Dill V, Franco AR, Pinho MS. Automated methods for hippocampus segmentation: the evolution and a review of the state of the art. *Neuroinformatics*. 2015;13:133–150.
30. Grimm O, Pohlack S, Cacciaglia R, et al. Amygdalar and hippocampal volume: a comparison between manual segmentation, Freesurfer and VBM. *J Neurosci Methods*. 2015;253:254–261.
31. Hu WH, Liu LN, Zhao BT, et al. Use of an automated quantitative analysis of hippocampal volume, signal, and glucose metabolism to detect hippocampal sclerosis. *Front Neurol*. 2018;9:820.